Article

Not peer-reviewed version

Toward Anode-Free Lithium-Ion Battery Using Amorphous Titanium Oxide Thin Films by Atmospheric-Pressure Mist Chemical Vapor Deposition

Hibiki Fukushima , Hajime Shirai * , Hirotaka Sone , Hideki Kurihara , Toshinori Ohno , Takuya Watanabe

Posted Date: 6 January 2025

doi: 10.20944/preprints202501.0376.v1

Keywords: Mist CVD; $Ti(acac)_2(OiPr)_2$; Amorphous TiO_x; LiTiO; Anode free LIB; Li ion diffusion

Article

Toward Anode-Free Lithium-Ion Battery Using Amorphous Titanium Oxide Thin Films by Atmospheric-Pressure Mist Chemical Vapor Deposition

Hibiki Fukushima [1], Hajime Shirai [1,*], Hirotaka Sone [1], Hideki Kurihara [2], Toshinori Ohno [3] and Takuya Watanabe [3]

[1] Graduate School of Science and Engineering, Saitama University

[2] Saitama Industrial Technology Center

[3] AMAYA CVD CO., LTD.

* Correspondence: shirai@fms.saiatma-u.ac.jp; Tel.: +81-048-858-3676

Abstract: We demonstrate the potential of Lithium titanate (LiTiO) and amorphous titanium oxide (a-TiO_x) thin films synthesized from titanium diisopropoxide bis acetylacetonate $C_{16}H_{28}O_6Ti$ [$Ti(acac)_2(OiPr)_2$] using atmospheric-pressure mist chemical vapor deposition method as negative electrode and solid electrolyte for anode-free lithium-ion battery (LIB). LTO thin films synthesized from $Ti(acac)_2(OiPr)_2$ and $LiNO_3$ at 500 ℃ act as a negative electrode in LIB. In a-TiO_x synthesized at 200-300 ℃, Li-ion permeability improved with charge/discharge cycles and acts as a solid electrolyte. The high diffusivity of Li ions demonstrated its superior behavior as a solid electrolyte. The a-TiO_x solid electrolyte battery achieved an charge/discharge efficiency of 94%. These results imply that a-TiO_x holds promise for realizing anode-free lithium metal batteries.

Keywords: Mist CVD; $Ti(acac)_2(OiPr)_2$; Amorphous TiO_x; LiTiO; Anode free LIB; Li ion diffusion

1. Introduction

Today, solid state lithium-ion battery (LIB) has been extensively studied for high energy density, high output characteristics, and excellent safety more than that of electrolyte solution based LIB. They are applied for use of micropower sources for smart cards, medical devices, micro electric mechanical system, wireless sensors and so on [1,2]. It has been reported that solid electrolytes with Li ion conductivity, such as perovskite crystals $Li_{0.35}La_{0.55}TiO_3$ [3] and $Na_{1+x}ZrSi_xP_{3-x}O_{12}$ ($0 < x < 3$) NASICON crystal structures, $Li_{1+x}Al_xTi_{2-x}(PO_4)_3$ exhibit ion conductivity of 10^{-4}~10^{-3} S/cm at room temperature [4]. However, these electrolytes have problems with poor stability and are electrochemically reduced at a potential of about 1.8 V vs. Li/Li^+, making it difficult to apply them as electrolytes for LIB secondary batteries. As electrolytes with wide potential windows, $Li_{0.35}La_{0.55}Zr_2O_{12}$ and lithium phosphate oxynitride glass (LiPON), which have a garnet structure [5–7], have been well-known. Also they include difficulties in the synthesis and LIB fabrication processes, so further technological development is required in the future. In recent years, it has been reported that sulfide-based compounds exhibit high Li^+ ion conductivity and can be applied to all-solid-state LIBs, and research and development have been actively underway. Sulfide ions have a higher polarizability than oxide ions, and the structure of the solid electrolyte is easily distorted when Li^+ diffuses [8,9], so it has superior Li^+ diffusion ability. Recently, highly conductive electrolytes such as sulfide-based crystalline $Li_{10}GePsS_{12}$ (approximately 10^{-2} S/cm at room temperature) have also been reported [10]. However, since sulfide electrolytes easily react with moisture in the atmosphere to produce H_2S, improving their chemical stability is an issue that must be overcome [11–14]. As one of the breakthroughs, the chemically stable oxide-based crystallized as well as amorphous all-solid-state

 doi:10.20944/preprints202501.0376.v1

batteries are a possible candidate, but the synthesis of the solid electrolyte and the defect-free negative electrode/electrolyte interface is still crucial to overcome because if even a small amount of current concentration occurs in an electrolyte, lithium metal grows in a dendrite pattern, causing partial short circuits and cycle deterioration (Figure S1). A certain amount of lithium metal was deposited (charged) and the coulombic charge/discharge efficiency was determined from the amount dissolved (discharged). Thus, this is an evaluation of anode-free lithium metal electrodes. For further development of LIB with excellent functionality, higher Li ion mobility of Li^+ in the electrolyte and faster desolvation of solvated Li^+ at the electrode interface is required using a uniform solid electrolyte thin film that conducts lithium ions without any current concentration at the anode/negative electrode.

Several methods have been employed for thin film deposition using vacuum-based and solution process techniques [15] like sputtering [16–18], spray coating [19], plasma sintering [20], chemical vapor deposition (CVD) [21], atomic-layer deposition [22–24], plasma-enhanced CVD (PE-CVD) [25], sol-gel [26,27], and mist CVD [28–30]. Among these, mist CVD is a possible candidate for preparing a variety of metal oxide thin films with no use of complex components from cost-effective, chemically stable, and low vapor pressure materials such as metal acetylacetonate $Ti(acac)_2(OiPr)_2$ and $Al(acac)_3$. In this process, the film is grown via the thermal decomposition of the source material, dissolved in a solvent such as H_2O and CH_3OH. We have studied the synthesis of amorphous (a-) AlO_x and a-TiO_x thin films by mist CVD and found that the dense a-AlO_x, a-TiO_x, and a-$Al_{1-y}Ti_yO_3$ network with smooth surface, and higher refractive index was obtained by tuning deposition parameters, i.e., furnace temperature T_f, carrier gas flow, $Ti(acac)_2(OiPr)_2/CH_3OH$ solute concentration, mesh bias and so on [31–34]. However, there are only a few studies on the mist CVD to LIB-related material synthesis and device manufacturing processes [35–37].

In this paper, we demonstrate the synthesis of lithium titanate $Li_4Ti_5O_{12}$ and a-TiO_x thin films from aqueous solution $Ti(acac)_2(OiPr)_2$ via mist CVD and they provide great potential as negative electrodes for LIB and solid electrolyte material for realizing anode-free LiB.

2. Materials and Methods

Figure 1(a) shows the molecular structure of $Ti(acac)_2(OiPr)_2$ and the setup of the mist-CVD apparatus used in this study, comprising an atomizer (operating at 2.4 MHz), Si tube, shower head nozzle (12 cm length, 3 mm gap), and operation substrate stage. The distance between the substrate and the tip of the shower nozzle is 3 mm. The substrate stage was operated at 5 mm/s and the film thickness was adjusted by the number of repetition cycles as a variable. The layer thickness per cycle was 3-3.3 nm/cycle and the total film thickness was 30-100 nm. The solution of 0.015 mol/L $Ti(acac)_2(OiPr)_2$ diluted in CH_3OH with and without adding Li source ($LiNO_3$, $Li(CH_3COO)$, LiCl) as a guest Li source for LTO and a-TiO_x thin films, respectively. They were set on an atomizer (2.4 MHz) and $Ti(acac)_2(OiPr)_2$ mist was generated and transported through a Si tube with an inner diameter of 20 mm using N_2 or Ar as a carrier gas. They were supplied from the shower nozzle to the substrate on the movable stage. The films were synthesized on crystalline Si, SUS coin cell, and copper foil (15~18 μm thickness) placed on a movable stage. The deposition condition of LTO and a-TiO_x is summarized in **Table 1**. The film thickness was adjusted at approximately 100 nm by setting the repetition cycle of the movable stage at 5 mm/s and T_s. **Figure 1(b)** shows the schematic of the LIB structure based on crystalline amorphous LTO and a-TiO_x as solid electrolytes formed on the Cu foil. In conventional crystal phase electrolytes, Li ions are introduced depending on the plane orientation of the crystal, on the other hand, isotropic diffusion is expected in an amorphous structure due to disturbance of the network structure. The electrochemical evaluation was performed by creating a cell in which the prepared LTO or a-TiO_x thin films, polypropylene separator, electrolyte, and metallic lithium were placed in such a jig and performing a charge/discharge test and cyclic voltammetry (CV).

 doi:10.20944/preprints202501.0376.v1

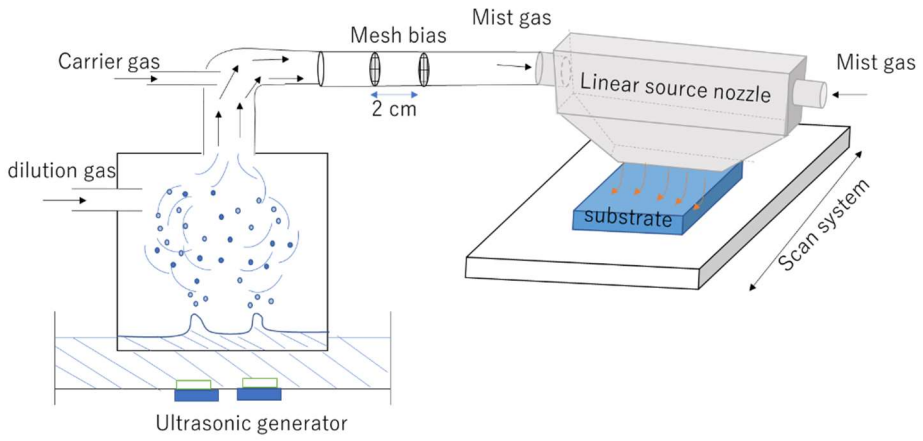

(**a**)

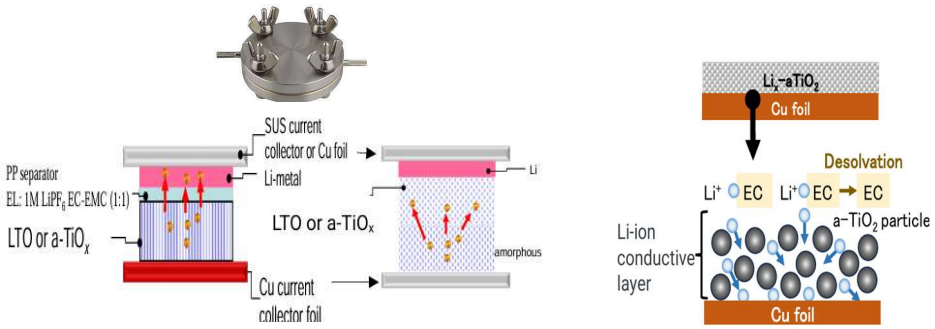

(**b**)

Figure 1. (a) Schematic of the mist CVD apparatus with linear source. (b) The LIB structure using crystalline LTO and a-TiO_x as solid electrolytes formed on the Cu foil. Schematic of Li-ion diffusion process in crystalline LTO and a-TiO_x particle.

Table 1. Deposition condition of LTO and a-TiO_x thin films.

Solute	$Ti(acac)_2(OiPr)_2$
Li source	$LiNO_3$, $(CH_3COO)Li$, LiCl
Solvent	CH_3OH
Solution concentration	0.015 mol/L
Substrate temperature; T_s	LTO; 500- 550 ℃, a-TiO_x; 200- 350 ℃
Substrate	p-Si, SUS, Cu foil (180 μm)
Mist generation gas	N_2, Ar: 500 sccm
Dilution gas flow; F_d	N_2, Ar: 2400 sccm
Repetition cycle; *N*	1 - 30

The LTO and a-TiO_x films were characterized by X-ray diffraction (XRD) and electrochemical evaluation. First, we investigated the synthesis of $Li_4Ti_5O_{12}$ thin films by adding guest Li sources [$LiNO_3$, $(CH_3COO)Li$, LiCl] to the film deposition condition of a-TiO_x thin films used in the previous study [31–34]. After that, post-annealed at 300- 500 °C for 30 min was performed to promote the film crystallization. Furthermore, the refractive index and extinction coefficient (*n*, *k*) spectra of a-TiO_x thin films prepared at different substrate temperatures T_s were measured using spectroscopic ellipsometry (Uvisel2, HORIBA) using the Tauc–Lorentz model combined with the two-layer model.

3. Results and Discussion

 doi:10.20944/preprints202501.0376.v1

Figure 2(a) shows the XRD pattern of a 100-nm thick LTO film with $LiNO_3$ synthesized T_s at 500 °C. The XRD diffraction peaks observed at around 2θ = 19° and 25° correspond to LTO (111) and TiO_2 (101) orientation, respectively, [35–37] suggesting that the film structure was a mixture of LTO and TiO_2. In addition, at a T_s of 200-350°C, no peaks appeared, indicating that the film is an amorphous state. The XPS revealed that the LTO film composition was Ti (19.5 at%), O (50.9 at%), Li (3.7 at%), and C (15.7 at%), suggesting far from stoichiometric composition $Li_4Ti_5O_{12}$. As-deposited a-TiO_x at T_s of 200-350 °C was Ti (18.6 at%), O (47.6 at%), and C (33 at%), suggesting that a-TiO_x includes huge C content.

Figure 2(b) shows the n and k spectra of a-TiO_x synthesized at different T_s. The magnitude of n and k values increase systematically with a slightly higher energy shift of absorption edge in k spectra when T_s was increased from 200 to 350 °C, and their values are lower than those of anatase rutile crystalline. These will be caused by a large amount of residual C, CHO, and COOH-related complex, although the influence on the LIB performance is still controversial. These a-TiO_x thin films are less dense and have more vacancies in their network than the anatase and rutile crystal structures.

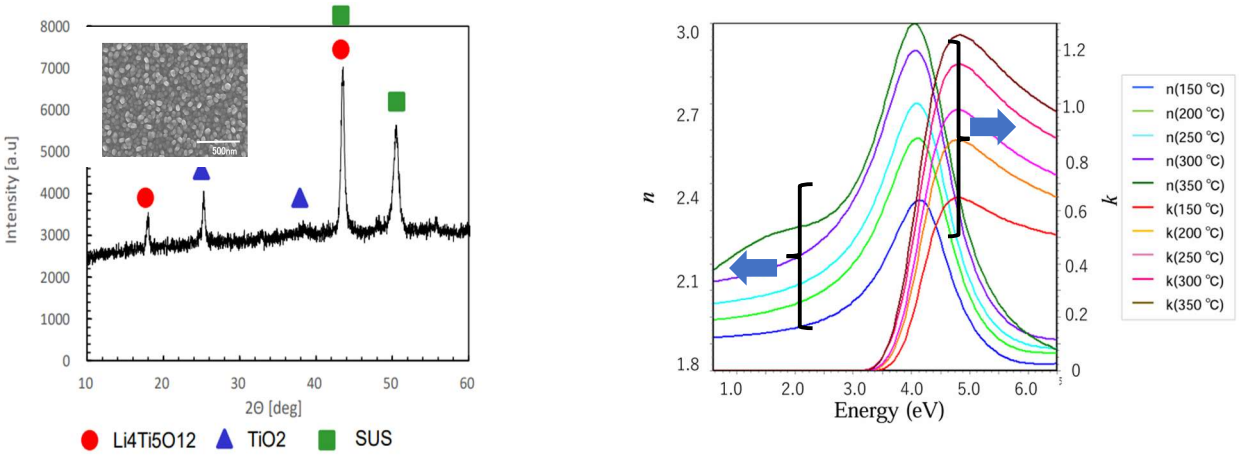

(**a**) (**b**)

Figure 2. (a) XRD pattern of LTO synthesized from $Ti(acac)_2(OiPr)_2$ and $LiNO_3$ mixture solution at a T_s of 500°C. The inset shows the SEM image of corresponding a-TiO_x and LTO (b) (n, k) spectra of a-TiO_x synthesized at different T_s from a 0.015M $Ti(acac)_2(OiPr)_2$ diluted in CH_3OH using mist CVD.

Figures 3(a) and (b) show the charge/discharge curve and CV characteristic of an LTO thin film including TiO_x phase fabricated at a T_s of 500 °C. In the charge-discharge curve, an irreversible capacity was detected at the first cycle, but stable redox behavior with no irreversible capacity was observed. The CV chracteristics of Li_x-a-TiO_x thin film with and without cleaning by acetone is aslo shown in Figure S2.These results suggest that the insertion and desorption of Li ions are stable after the initial insertion of Li ions from the second cycle onwards. In CV, reduction peaks were detected around 1.7V and 1.5V. This is presumed to be due to the reduction reaction of TiO_x and LTO (Figure S3).

The redox potential of LTO is approximately 1.8-1.9V (Figure 3b), which is higher than that of $Li_4Ti_5O_{12}$ (1.56V) due to smaller Li content [38–40]. Additionally, an oxidation peak was detected around 2.2V.

Preprints.org (www.preprints.org) | NOT PEER-REVIEWED | Posted: 6 January 2025 doi:10.20944/preprints202501.0376.v1

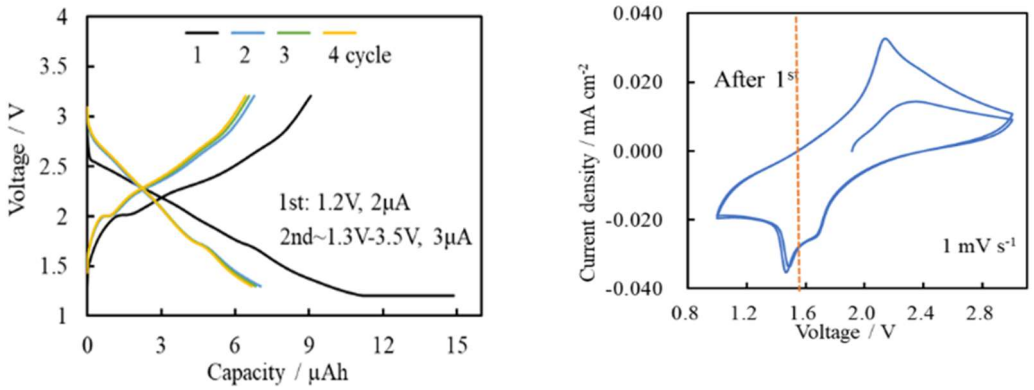

(**a**) (**b**)

Figure 3. (a) Charge/discharge and (b) CV characteristics of a LTO thin film containing TiO_2 anatase phase synthesized at a T_s of 500 °C by mist CVD.

Figure 4(a) and (b) show the charge/discharge and CV curves of a-TiO_x thin films synthesized at T_ss of 200- 350 °C. The charge-discharge curve revealed that the capacity is higher compared to LTO films synthesized at a T_s of 500 ℃. Additionally, the coulombic efficiency was increased due to the increase in oxidation capacity with the cycles. This result suggests that Li-ion is easily desorbed during charging and discharging, and the permeability of Li ions is improved. Furthermore, no peaks for oxidation/reduction reactions were detected in the CV curve. These findings suggest that Li ions are not inserted into a predetermined crystal structure, but rather diffused into arbitrary positions in the amorphous structure. These results imply that the amorphous TiO_x has higher Li-ion permeability than the crystalline structure. This is because Li ions can diffuse isotopically in an amorphous network, while they move in a specific direction depending on the crystal plane in a crystalline structure. Thus, these results imply that a-TiO_x is expected to act as a solid electrolyte.

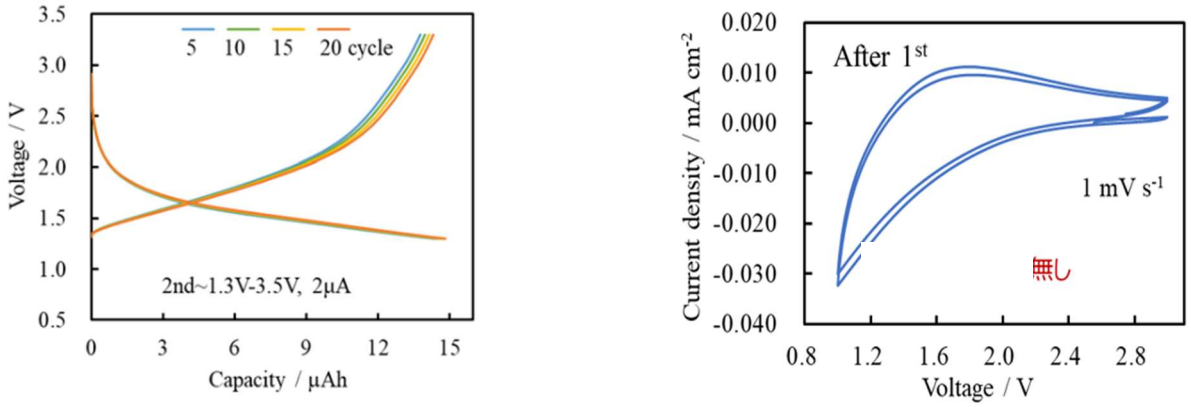

(**a**) (**b**)

Figure 4. (a) Charge/discharge and (b) CV characteristic for a-TiO_x fabricated at T_s of 200-350 °C using mist CVD.

Furthermore, the a-TiO_x thin films synthesized at a T_s of 200°C were scanned to the potential at which Li was deposited. The charge/discharge curve and CV are also shown in Figure 5a. In the charge/discharge test, the battery was charged to 2.5 $mAhcm^{-2}$, which has a similar potential to widely used electrodes, and discharged to 1.0V. It is noted that the Li's precipitation and dissolution behavior were detected. The coulombic efficiency was 94%. The remarkable redox behavior of Li precipitation and dissolution was also detected in CV (Figure 5b). The current density increased with cycling. This is presumed to be because the permeability of lithium ions increased with cycling. These results suggest that in reduction, Li ions pass through the a-TiO_x thin film and Li metal precipitates on the

Preprints.org (www.preprints.org) | NOT PEER-REVIEWED | Posted: 6 January 2025 doi:10.20944/preprints202501.0376.v1

Cu current collector foil, and in oxidation, Li ions dissolve from the Li metal on the Cu foil and pass through the a-TiO_x thin film. Additionally, no micro-short circuit behavior during Li precipitation occurred in a series of measurements. These findings imply that a-TiO_x thin film has the potential to realize an anode-free lithium metal battery. The theoretical capacity of $Li_4Ti_5O_{12}$ is 175 mAh/g, but for LTO synthesized by mist CVD from $Ti(acac)_2(OiPr)_2$ at 500 °C is initial 300 mAh/g, second 150 mAh/g, and 300 mAh/g for a-TiO_x at 300 °C. These results suggest that a-TiO_x from $Ti(acac)_2(OiPr)_2$ by mist CVD provides higher capacity. Furthermore, the weight per unit area of a 200-nm thick a-TiO_x thin film is approximately 0.1mg/cm², and no binder or conductive additive is required in the LIB manufacturing process. On the other hand, electrodes synthesized using other coating processes are equivalent to 0.02 g/cm² at a thickness of 2 μm, and contain 70-90% of the active material, binder, conductive aid, etc. Therefore, although TiO_x produced by the mist CVD method shows an amorphous state, its density is approximately 1/10 that of electrodes produced using a conventional coating press. These results suggest that mist CVD a-TiO_x is a likely anode-free LIB due to the simple process.

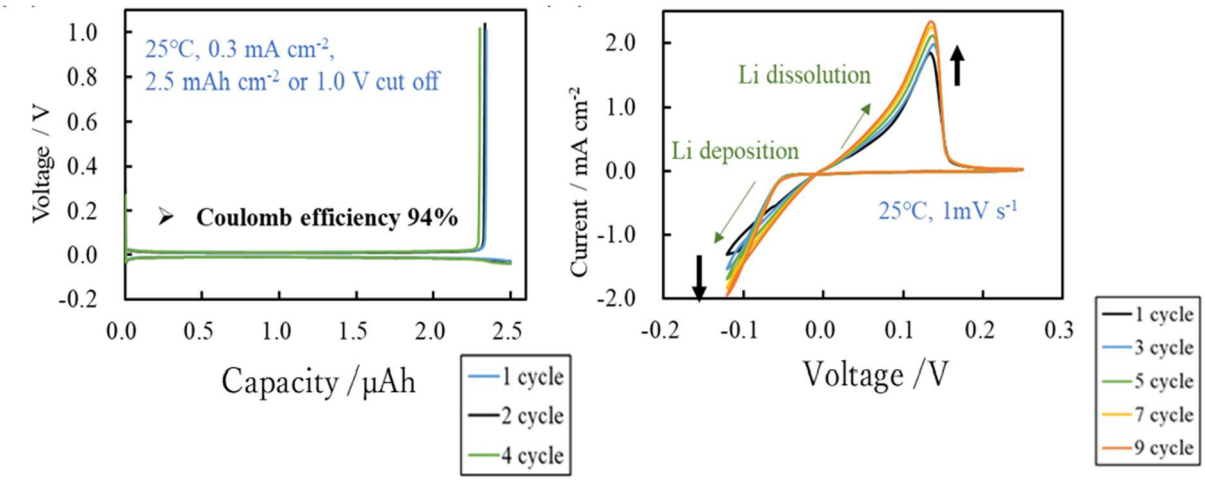

(a) (b)

Figure 5. (a) Charge/discharge and (b) CV curves of a-TiO_x synthesized at a T_s of 200 ℃.

Anode-free lithium metal batteries utilize Li metal as the negative electrode, which provides optimal performance because Li metal is not present during battery manufacturing, thus achieving high safety and low cost. Cu foil, and when using crystalline TiO_x electrodes, Li-ion is trapped, and charging becomes impossible. Further detailed studies are underway, but there are challenges to realizing it. Therefore, these results could be a major step in realizing anode-free lithium metal batteries [41,42].

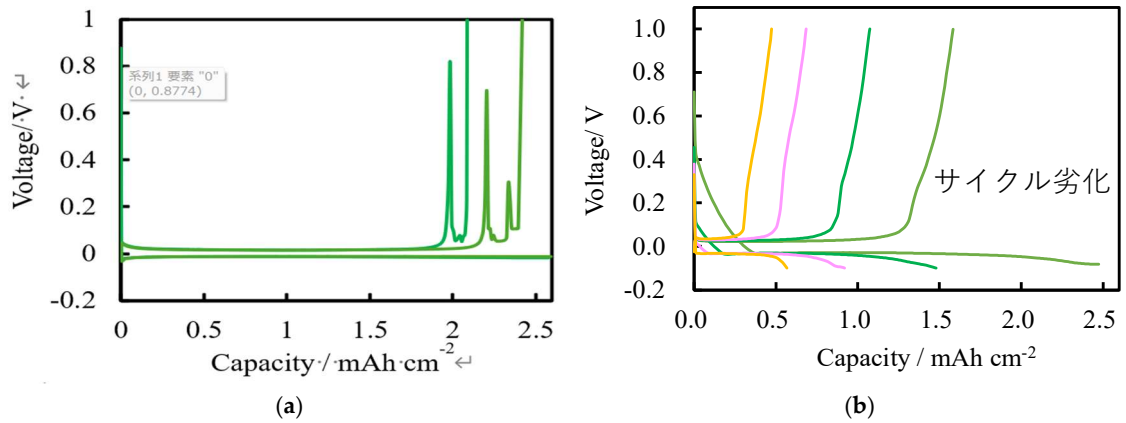

(a) (b)

Figure 6. (a) Charge discharge curve of (a) Cu foli alone/Li and (b) crystalline TiO_x particle/Li metal.

 doi:10.20944/preprints202501.0376.v1

5. Conclusions

We investigated the synthesis of lithium titanate (LTO) and a-TiO_x thin films from $Ti(acac)_2(OiPr)_2$ diluted in CH_3OH by mist CVD and applied in negative electrode and electrolyte of LIB. LTO synthesized at 500 ℃ comprises crystalline LTO that acts as a negative electrode material. A-TiO_x synthesized at 250-300 ℃ improved the Li-ion permeability with charge/discharge cycles, and they also exhibit superior behavior as a solid electrolyte due to the high diffusivity of Li ions. The corresponding LIB with a-TiO_x as a solid electrolyte showed a charge/discharge efficiency of 94%. These findings suggest that a-TiO_x by mist CVD as solid-electrolyte holds promise for realizing anode-free lithium metal batteries.

Supplementary Materials: The following supporting information can be downloaded at: www.mdpi.com/xxx/s1, **Figure S1:** (a) Remaning issue for anode-free Li_x-aTiO_2 LIB. (b) Microsocpe image of Li_x-aTiO_2 after charge/discharge cycles. **Figure S2**: Effect of a-TiO_x film thickness and cleaning by immersion in acetone on CV (Li precipitation-dissolution behavior) of Li-a-TiO_x/Cu-Li metal. **Figure S3**: SEM image of Li_x-a-TiO_x before and after charge/discharge cycles.

Author Contributions: Synthesis of a-TiO_x and LTO films by mist CVD, H. Fukushima and H. Watanabe, LIB device fabrication and evaluation; H. Kurihara.; investigation, H. Shirai and H. Sone.; original draft preparation, H. Shirai; writing—review and editing, H. Sone;. project administration and funding acquisition, T. Ohno. All authors have read and agreed to the published version of the manuscript.

Funding: This study is partially supported by the Circular Economy Business Development Grant of Saitama Pref. FY2023.

Data Availability Statement: We encourage all authors of articles published in MDPI journals to share their research data. In this section, please provide details regarding where data supporting reported results can be found, including links to publicly archived datasets analyzed or generated during the study. Where no new data was created, or where data is unavailable due to privacy or ethical restrictions, a statement is still required. Suggested Data Availability Statements are available in the section "MDPI Research Data Policies" at https://www.mdpi.com/ethics.

Acknowledgments: The authors appreciate Mrs. Y. Wasai and Mr. Y. Izumi (HORIBA Techno Service Co., Ltd) for supporting the ellipsometry measurement.

Conflicts of Interest: The authors declare no conflicts of interest associated with this manuscript. All authors approved the final version of the manuscript. (H. Fukushima, H Shirai, H. Kurihara, H. Sone, T. Ohno, T. Watanabe).

References

1. Yang, G.; Abrahama, C.; Ma, Y.; Lee, M.; Helfrick, E.; Oh, D.; Lee, D. Advances in Materials Design for All-Solid-state Batteries: From Bulk to Thin Films. *Appl. Sci.* **2020**, *10*(14), 4727; https://doi.org/10.3390/app10144727
2. Cao, C.; Li, Z-B.; Wang, X-L.; Zhao, X-B.; Han, W-Q. Recent Advances in Inorganic Solid Electrolytes for Lithium Batteries *Frontier Energy Res*. **2014.** 27 Sec. Electrochemical Energy Storage Volume 2 https://doi.org/10.3389/fenrg.2014.00025
3. M. Yashima, M. Itoh, Y. Inaguma, and Y. Morii, **Crystal Structure and Diffusion Path in the Fast Lithium-Ion Conductor $La_{0.62}Li_{0.16}TiO_3$.** *J. Am. Chem. Soc.* **2005**, 127, 3491-3495. doi: 10.1021/ja0449224
4. J. Fu, Fast Li^+ ion conducting glass-ceramics in the system Li_2O – Al_2O_3 – TiO_2 – SiO_2 – P_2O_5. *J. Am. Ceram. Soc*. 80, 1901 (1997).
5. R. Murugan, V. Thangadural, and W. Weppner, Fast Lithium Ion Conduction in Garnet-type $Li_7La_3Zr_2O_{12}$. *Angew. Chem. Int*. Ed,. **2007**, 46, 7778. doi: 10.1002/anie.200701144

6. B. Wang, J. B. Bates, F. X. Hart, B. C. Sales, R. A. Zuhr, and J. D. Robertson, Characterization of Thin-Film Rechargeable Lithium Batteries with Lithium Cobalt Oxide Cathodes. *J. Electrochemical. Soc*., **1996**, 143, 3203. **doi** 10.1149/1.1837188
7. S. Ohta, T. Kobayashi, J. Seki, T. Asaoka, Electrochemical Performance of an All-solid-state Lithium Ion Battery with Garnet-Type Oxide Electrolyte. *J. Power Sources*, **2012**, 202, 332–335. https://doi.org/10.1016/j.jpowsour.2011.10.064
8. R. Kanno, M. Murayama, Lithium Ionic Conductor Thio-LISICON: The Li_2S GeS_2 P_2S_5 System. *J. Electrochem. Soc.* **2001**, 148, A742. **doi** 10.1149/1.13790288
9. Kato, Y.; Hori, S.; Saito, T.; Suzuki, K.; Hirayama, M.; Mitsui, A,; Yoneyama, M.; Iba, H.; Kanno, R. High-power All-solid-state Batteries using Sulfide Superionic Conductors. *Nature Energy* **2016**, 1, 16030. https://ui.adsabs.harvard.edu/link_gateway/2016NatEn...116030K/doi:10.1038/nenergy.2016.30
10. N. Kamaya, K. Homma, Y. Yamakawa, M. Hirayama, R. Kanno, M. Yonemura, T. Kamiyama, K. Kato, S. Hama, K. Kawamoto, and A. Mitsui, A Lithium Superionic Conductor. *Nat. Mater.* **2011**, 10, 682-686. doi.org/10.1038/nmat3066
11. A. Hayashi, S. Hama T. Minami, and M. Tatsumisago, Fast Lithium-Ion Conducting Glass-Ceramics in the System Li_2S-SiS_2-P_2S_5. *Electrochem. Commun*. **2003**, 5, 111-114.
12. S. Nishimura, N. Tanibata, A. Hayashi, M. Tatsumisago, A. Yamada The Crystal Structure and Sodium Disorder of High-Temperature Polymorph β-Na_3PS_4**.** *J. Mater. Chem.* A., **2017**, **5**, 25025-25030. https://doi.org/10.1039/C7TA08391B
13. T. Hakari, Y. Sato, S. Yoshimi, A. Hayashi, M. Tatsumisago Favorable Carbon Conductive Additives in Li_3PS_4 Composite Positive Electrode Prepared by Ball-Milling for All-Solid-State Lithium Batteries *J. Electrochem. Soc*., **2017**, 162 (12), A2804-A2811. **DOI** 10.1149/2.1831712jes
14. A. Sakuda, A. Hayashi, M. Tatsumisago Recent Progress on Interface Formation in All-Solid-State Batteries. *Curr. Opin. Electrochem.,* **2017**, 6, 108-114.
15. Perkins, C. Y.; Mansergh, R. H.; Ramos, J. C.; Nanayakkara, C. E.; Park, D. -H.; Ferron, S. G.; Fullmer, L. B.; Arens, J. T.; Gutierrez-Higgins, M. T.; Jones, Y. R.; Lopez, J. I.; Rowe, T. M.; Whitehurst, D. M.; Nyman, M.; Chabal, Y. J.; Keszler, D. A. Low-index, Smooth Al_2O_3 Films by Aqueous Solution Process, *Optical Material Express* **2017**, *7*, 273-278. doi.org/10.1364/OME.7.000273
16. Alberti, A.; Smecca, E.; Sanzaro, S.; Bongiorno, C.; Giannazzo, F.; Mannino, G.; Magna, A. L. Nanostructured TiO_2 Grown by Low-Temperature Reactive Sputtering for Planar Perovskite Solar Cells. *ACS Appl. Energy Mater.* **2019**, *2*, 6218-6229. doi.org/10.1021/acsaem.9b00708
17. Dai, H. -Q.; Xu, H.; Zhou, Y. -N.; Lu, F.; Fu, Z. -W. Electrochemical Characteristics of Al_2O_3-Doped ZnO Films by Magnetron Sputtering. *J. Phys. Chem. C* **2012**, *116*, 1519-1525. doi.org/10.1021/jp208745n
18. K.H. Hwang, S.H. Lee and S.K. Joo, Characterization of Sputter-deposited $LiMn_2O_4$ Thin Films for Rechargeable Microbatteries. *J. Electrochem. Soc.* **1994**, 141, 3296-3299. IP 130.203.136.75
19. Shamala, K. S.; Murthy, L. C. S.; Radhakrishna, M. C.; Rao, K. N. Characterization of Al_2O_3 Thin Films Prepared by Spray Pyrolysis Method for Humidity Sensor. *Sens. Actuators A* **2007**, *135*, 552-557. doi:10.1016/j.sna.2006.10.004
20. A. Mei, Q. H. Jiang, Y. H. Lina, C. W. Nan, Lithium Lanthanum Titanium Oxide Solid-State Electrolyte by Spark Plasma Sintering. *J. Alloys Compounds* **2009**, 486, 871–875.
21. Lei, L.; Chu, H. P.; Hu, X.; Yue, P. -L. Preparation of Heterogeneous Photocatalyst (TiO_2/Alumina) by Metal-Organic Chemical Vapor Deposition. *Ind. Eng. Chem. Res.***1999**, *38*, 3381-3385.
22. Chung, H. K.; Won, S. O.; Park; Y.; Kim, J.; Park, T. J.; Kim, S. K. Atomic-layer deposition of TiO_2 Thin Films with a Thermally Stable $(CpMe_5)Ti(OMe)_3$ Precursor. *Appl Surf Sci.* **2021**, 550, 149381. doi.org/10.1016/j.apsusc.2021.149381
23. Roelofs, K. E.; Brennan, T. P.; Dominguez, J. C.; Bailie, C. D.; Margulis, G. Y.; Hoke, E. T.; McGehee, M. D.; Bent, S. F. Effect of Al_2O_3 Recombination Barrier Layers Deposited by AtomicLayer Deposition in Solid-State CdS Quantum Dot-Sensitized Solar Cells. *J. Phys. Chem. C* **2013**, *117*, 5584-5592. doi.org/10.1021/jp311846r

24. Wan, Z.; Zhang, T. F.; Lee, H. -B. R.; Yang, J. H.; Choi, W. C.; Han, B.; Kim, K. H.; Kwon, S. -H. Improved Corrosion Resistance and Mechanical Properties of CrN Hard Coatings with an Atomic Layer Deposited Al_2O_3 Interlayer. *ACS Appl. Mater. Interfaces* **2015**, *7*, 26716-26725. doi.org/10.1021/acsami.5b0869
25. Chrysson, C. E.; Pitt, C.W. Al_2O_3 Thin Films by Plasma-Enhanced Chemical Vapour Deposition Using Trimethyl-Amine alane (TMAA) As the Al Precursor. *Appl. Phys. A* **1997**, *65*, 469-475. doi.org/10.1007/s003390050611
26. Rho, Y.H.; Kanamura, K. Fabrication of thin film Electrodes for All Solid State Rechargeable Lithium Batteries, *J. Electroanal. Chem*. **2003**, 559, 69-75.
27. Rho, Y.; Kanamura, K.; *J. Solid State Chem*. **2003**, 559, 69-75.
28. Oh, K. -T.; Kim, H. -Y.; Kim, D. -H.; Hwan Han, J. H.; Park, J.; Park, J. -S. Facile Synthesis of AlO_x Dielectrics via Mist-CVD Based on Aqueous Solutions. *Ceram. Int.* **2017**, *43*, 8932-8937. doi.org/10.1016/j.ceramint.2017.04.031
29. Uchida, T.; Kawaharamura, T.; Shibayama, K.; Hiramatsu, T.; Orita, H.; Fujita, S. Mist Chemical Vapor Deposition of Aluminum Oxide thin Films for Rear Surface Passivation of Crystalline Silicon solar cells. *Appl. Phys. Express* **2014**, *7*, 021303. **doi** 10.7567/APEX.7.021303
30. Kawaharamura, T.; Uchida, T.; Sanada, M.; Furuta, M. Growth and Electrical Properties of AlO_x Grown by Mist Chemical Vapor Deposition. *AIP Adv.* **2013**, *3*, 032135. doi.org/10.1063/1.4798303
31. Rajib, A.; Enamul, K.; Kuddus, A.; Ishikawa, R.; Ueno, K.; Shirai, H, Synthesis of AlO_x Thin Films by Atmospheric-pressure Mist Chemical Vapor Deposition for Surface Passivation and Electrical Insulator Layers, *Journal Vacuum Science & Technology* **2020**, A38, 033413. **doi**.org/10.1116/1.5143273
32. Rajib, A.; Kuddus, A.; Shida, T.; Ueno, K.; Shirai, H. Mist Chemical Vapor Deposition of AlO_x Thin Films Monitored by a Scanning Mobility Particle Analyzer and its Application to the Gate Insulating Layer of Field-effect Transistors. *ACS Applied Electronic Materials* **2021**, *3*, 658–667. doi.org/10.1021/acsaelm.0c00758
33. A. Rajib, A. Kuddus, K. Yokoyama, T. Shida, Ueno, K.; Shirai, H. Mist Chemical Vapor Deposition of $Al_{1-x}Ti_xO_y$ Thin Films and Their Application to a High Dielectric Material. *J. Applied Physics*. **2022,** *131*, 105301. doi.org/10.1063/5.0073719
34. Yokoyama, K.; Kuddus, A.; Shirai, H. Mesh-bias Controlled Synthesis of TiO_2 and $Al_{0.76}Ti_{0.24}O_3$ Thin films by Mist Chemical Vapor Deposition and Applications as Gate Dielectric Layers for Field-Effect Transistors. *ACS Applied Electronic Mater*. **2022**, 4(5), 2516-2524. doi:10.1021/acsaelm.2c00286
35. Tadanaga, K.; Yamaguchi, A.; Hayashi, A.; Tatsumisago, M.; Mosa, J.; Aparicio, M. Preparation of $Li_4Ti_5O_{12}$ electrode thin films by a mist CVD process with aqueous precursor solution. *J. Asian Ceramic Soc*., **2015**, 3, 88-91. doi.org/10.1016/j.jascer.2014.11.003
36. Tadanaga, K.; Yamaguchi, A.; Sakuda, A.; Hayashi, A.; Tatsumisago, Duran, A.; Aparicio, Preparation of $LiMn_2O_4$ Cathode Thin Films for Thin Film Lithium Secondary Batteries by a Mist CVD Process. *Mater. Res. Bul*. **2014**, **53**, 196-198. *https://doi.org/10.1016/j.materresbull.2014.01.032.*
37. Igawa, T.; Kaneko, K.; Fujita, S. Fabrication of Lithium-based Oxide Thin Films by Ultrasonic-Assisted Mist CVD Technique. *J. Soc. Mater. Sci., Japan* **2011**, 60, 994-997. In Japanese
38. Hirayama, M.; Kim, K.; Toujigamori, T.; Cho, W.; Kanno, R. Epitaxial growth and electrochemical properties of $Li_4Ti_5O_{12}$ thin-film lithium battery anodes. *Dalton Trans*. **2011**, **40**, 2882-2887. https://doi.org/10.1039/C0DT01477J
39. Ohzuku, K.; Ueda, A.; Yamamoto, N. Zero-Strain Insertion Material of $Li[Li_{1/3}Ti_{5/3}]O_4$ for Rechargeable Lithium Cells. *J. Electrochem.Soc*. **1995**, 142, 1431-1435. doi: 10.1149/1.2048592
40. Amine, K.; Belharouak, I.; Chen, Z.; Tran, T.; Yumoto, H. Ota, N.; Myung, S.T.; Sun Y.K. Nanostructured Anode Material for High-power battery System in Electric Vehicles. *Adv. Mater.* **2010**, 22, 3052-3057. doi: 10.1002/adma.201000441
41. Wang, C.; Liu, M.; Thijs, M.; Ooms, F.G.B.; Ganapathy, S.; Wagemaker, M. High Dielectric Barium Titanate Porous Scaffold for Efficient Li Metal Cycling in Anode-free cells. *Nat. Commun*. **2021**, 12, 6536. **doi:** 10.1038/s41467-021-26859-8
42. Wang, M.; Cheng, X.; Cao, T.; Niu, J.; Wu, R.; Liu X. Zhang, Y. Constructing ultrathin TiO_2 protection layers via atomic layer deposition for stable lithium metal anode cycling, *Journal of Alloys and Compounds* **2021**, 865, 158748. doi:10.1016/j.jallcom.2021.158748

 doi:10.20944/preprints202501.0376.v1